High-permittivity silicone dielectric elastomers compatible with ionic liquid-grafted chloropropyl-silicone oil

Zhaoqing Kang[a,b], Liyun Yu[a], Yi Nie[b], Suojiang Zhang[b], Anne Ladegaard Skov[*a]
[a]Danish Polymer Center, Department of Chemical and Biochemical Engineering, Technical University of Denmark, Kgs. Lyngby, Denmark; [b]CAS Key Laboratory of Green Process and Engineering, Beijing Key Laboratory of Ionic Liquids Clean Process, State Key Laboratory of Multiphase Complex Systems, Institute of Process Engineering, Chinese Academy of Sciences, Beijing, China

ABSTRACT

Dielectric elastomers (DEs) can undergo very large spatial deformations in response to an externally applied electrical field, giving them significant potential as soft actuators. High-performance DEs are usually modified by high-permittivity additives, which are used to lower driving voltages. In this study, a novel high-permittivity soft additive (LMS-EIL) was developed via the combination of high-permittivity ionic liquid (IL) and chloropropyl-silicone, enabling good compatibility with the silicone matrix. The relative dielectric permittivity of the novel silicone oil additive was 9×10^4 times higher at 0.1Hz compared to pristine chloropropyl-silicone oil. High-permittivity silicone elastomers were then achieved via incorporation of this novel IL-grafted chloropropyl-silicone oil. The relative dielectric permittivity of elastomers modified with 10 parts per hundred rubber (phr) LMS-EIL increased from 3.0 (pure film) to 22 at 0.1Hz, while the Young's modulus decreased steadily with increasing LMS-EIL concentration. A simplified figure of merit (F_{om}') was used to evaluate actuation performance, and was shown to be 8.1 for the elastomer incorporated with 10 phr LMS-EIL, indicating excellent potential for use as an actuator.

Keywords: dielectric elastomer, ionic liquids, high-permittivity, grafting, chloropropyl-silicone

1. INTRODUCTION

Dielectric elastomers (DEs) are promising soft electroactive materials[1], which can significantly alter their size or shape in response to an external electrical field[2]. Due to their low weight, low cost, fast response, and high efficiency[3], DEs are widely used in transducers such as artificial muscles[4], energy harvesters[5], and haptic devices[6]. DEs consist of an elastomer film sandwiched between two compliant electrodes, thereby creating a capacitor capable of energy transduction. When an electric field is applied through the electrodes, the elastomer deforms under Maxwell stress introduced by the electrostatic forces[7]. Polydimethylsiloxane (PDMS) elastomers are promising materials for dielectric elastomer transducers due to their excellent properties, such as high efficiency, reliability, and fast response times.[1, 8-10] However, their major disadvantage is that they require high driving voltages to actuate (typically 500 V to 10 kV) due to their relatively low dielectric permittivity[11], and thus limiting their use in DE applications.

One efficient method for improving actuation performance is to increase the relative dielectric permittivity of PDMS elastomers by adding high-permittivity additives, such as titanium oxide, zink oxide, aluminium oxide, or carbon nanotubes, to the matrix.[12-15] Although the incorporation of rigid additives can indeed increase the relative dielectric permittivity, some undesired side effects will also appear, such as high dielectric losses, low breakdown strengths, and high Young's moduli; and a large increase in Young's modulus can lessen or even eliminate the improvement in actuation due to relative dielectric permittivity. Additionally, many commonly used additives are incompatible with PDMS elastomers, causing aggregation that compromises the elastomers' mechanical properties. In order to increase relative dielectric permittivity and reduce Young's modulus simultaneously, it is therefore necessary to find a new additive which is more compatible with PDMS elastomers.

Based on the "like dissolves like" rule, high-permittivity functional silicone oil can be used as a compatible soft additive to increase the relative dielectric permittivity and reduce the Young's modulus of PDMS elastomers[11, 16-17]. Liu et al.[18] have shown that elastomers with a high chloropropyl-functional silicone oil content possess significantly increased relative dielectric permittivity as well as a reduced Young's modulus. However, the high amount of liquid additive in the elastomer matrix also significantly decreased both its tensile and electric breakdown strengths. Generally, the higher

relative dielectric permittivity of the functional silicone oil, the more efficiently its addition improves the relative dielectric permittivity of a given PDMS elastomer, provided that the associated worsening of tensile and electric breakdown strengths, as well as physical incompatibility are not too large.

As eco-friendly chemical compounds[19], ILs possess advantageous properties such as high thermal stability[20] and high relative dielectric permittivity[21], and have shown promise as additives capable of improving the relative dielectric permittivity of PDMS elastomers, with Liu et al.[22] reporting that 1-butyl-3-methylimidazolium hexafluoroantimonate is the most suitable IL for this purpose. However, due to poor compatibility of the ILs with PDMS, they tend to aggregate in the elastomer matrix.

In this study, a novel high-permittivity soft additive compatible with PDMS elastomers is developed by grafting IL onto the side chain of chloropropyl functional silicone oil. The extent of chemical grafting of IL, relative dielectric permittivity, and loss tangent of the modified silicone oil are then analyzed. High-permittivity dielectric silicone elastomers are subsequently prepared via incorporation of the IL-grafted silicone oil, and the influence of soft additive concentration on relative dielectric permittivity, loss tangent, morphology, and mechanical properties is investigated. Finally, the improved actuator functionality of the elastomer materials is evaluated by measuring dielectric breakdown strength as well as a figure of merit (F_{om}').

2. EXPERIMENTAL

2.1 Materials

[14-16 %(chloropropyl)methylsiloxane]-dimethylsiloxane, LMS-152 (M_w = 8750 g mol^{-1}) was purchased from Gelest Inc. 1-ethylimidazole and toluene were obtained from Sigma-Aldrich Co., Ltd. Silanol-terminated polydimethylsiloxane, C2T (M_w = 22000 g·mol^{-1}) was acquired from Wacker Chemie AG. Trimethoxylsiloxane and dibutyltin diacetate (Sn catalyst) were purchased from Sika technology AG. Silicon dioxide amorphous hexamethyldisilazane-treated particle (SIS6962.0) was purchased from Fluorochem. All products were used without further purification.

2.2 Synthesis of the compatible high-permittivity soft additive

LMS-EIL was synthesized by a traditional nucleophilic substitution and purified by extraction. For synthesis, a flask was charged with LMS-152 (10.0 g, 1.14 mmol), 1-ethylimidazole (1.10 g, 11.42 mmol), and toluene (10 mL). The reaction mixture was deoxygenated by bubbling nitrogen through it for 10 min. The flask was then heated to 85°C and the reaction was carried out for 24 h, after which the reaction was stopped by cooling the flask to room temperature. The purification process was as follows: the initial product was obtained by removing toluene in a rotary evaporator; the product was then washed three times with ethyl acetate to extract the unreacted monomers; after evaporation, the final product was dried in a vacuum oven for 24 h.

2.3 Preparation of elastomers incorporated with LMS-EIL

C2T (5.00 g, 0.22 mmol), trimethoxylsiloxane cross-linker (0.10 g, 0.76 mmol), and treated silica particles (10 phr) were mixed using a dual asymmetric centrifuge at 3500 rpm for 3 min (FlackTek Inc. DAC 150.1 FVZ-K SpeedMixer). The catalyst dibutyltin diacetate (0.5 wt%) and soft additive LMS-EIL were then added, and the mixture was speed mixed again. The uniform mixture was then cast with a coating height of 300 μm onto a polyethylene terephthalate (PET) substrate by a film applicator (3540 bird, Elcometer, Germany). The coated samples were subsequently cured for 48 h in a humidity oven at 25°C and 80% relative humidity.

2.4 Characterization

Fourier transform infrared spectroscopy (FT-IR)
FT-IR spectra of the samples were acquired in the wavenumber range of 400–4000 cm^{-1} using a Nicolet iS50 FT-IR fitted with a diamond crystal attenuated total reflection accessory (ATR). All spectra were acquired via 32 scans at a resolution of 4 cm^{-1} and were baseline corrected.
Proton Nuclear magnetic resonance (^{1}H-NMR)
^{1}H-NMR experiments were performed on a Bruker 300 MHz spectrometer using 100 mg mL^{-1} solutions in deuterated chloroform ($CDCl_3$).
Optical microscopy
PDMS elastomer morphology was investigated by optical microscope (Leica DMLS microscope, Germany).
Tensile strength and Young's modulus

Sample tensile stress-strain behavior was tested using a material tester (Instron 3340 materials testing system, INSTRON, US) at room temperature. The samples were cut to 60 mm length and 6 mm width before being placed between two clamps and initially separated by a distance of 30 mm. The test specimen was elongated uniaxially at 10 mm min^{-1} with respect to length. Young's modulus was obtained from the tangent of the stress-strain curves at 10% strain. Three measurements were taken for each sample and then averaged.

Dielectric relaxation spectroscopy (DRS)

DRS of samples was performed using a Novocontrol Alpha-A high-performance frequency analyzer (Novocontrol Technologies GmbH & Co, Germany) with an electrical field of about a 1 V mm^{-1}, in the frequency range 10^{-1} to 10^{6} Hz, at room temperature. The diameter and thickness of the tested samples were 20 mm and 1 mm, respectively.

Electrical breakdown strength (E_{BD})

The electrical breakdown strength of the samples was tested on a custom-built device based on international standards (IEC 60243–1 (1998) and IEC 60243–2 (2001))[23]. Tests were performed by increasing the voltage (50-100 V per step) of the device at a rate of 0.5-1 steps s^{-1}. Sample thickness was measured using optical microscopy. The distance between the spherical electrodes was set to 95% of the obtained thickness to ensure that the spheres were in contact with the sample. Each sample was subjected to 12 breakdown measurements at room temperature, and the average of these values was given as the E_{BD} of the sample.

Figure of merit

The performance of dielectric elastomer actuators (DEAs) was evaluated using Equation (1), which is a so-called figure of merit (F_{om}) by Sommer-Larsen and Larsen[24]. This equation offers a guide for optimizing DEAs:

$$F_{om}(\text{DEAs}) = \frac{3\varepsilon_r\varepsilon_0 E_{BD}^2}{Y} \quad (1)$$

Here, ε_0 represents vacuum permittivity (8.85×10^{-12} F m^{-1}), ε_r represents the relative permittivity, and Y represents Young's modulus. In practical use, however, such as in the case of a particular battery providing a certain voltage and where the voltage applied on the DEAs is usually always lower than the E_{BD}, then the figure of merit for actuators in Equation (1) can be simplified to[9]:

$$F_{om}'(\text{DEAs}) = \frac{\varepsilon_r}{Y} / \frac{\varepsilon_{ref}}{Y_{ref}} \quad (2)$$

Where ε_{ref} is the relative permittivity of the reference material value and Y_{ref} is its Young's modulus. Compared to Equation (1), the ratio of relative permittivity to Young's modulus in this equation is an acceptable approximation for evaluating the improved actuation of a given elastomer actuated at a voltage below its E_{BD}.

3. RESULTS AND DISCUSSION

The resulting structure of elastomers incorporated with LMS-EIL is illustrated in Scheme 1. LMS-EIL is not chemically incorporated into the PDMS matrix, therefore IL-rich domains will be formed with a size that is mainly determined by the immiscibility between the IL groups and PDMS while the PDMS part of the LMS-EIL will ensure overall compatibility. The cross-linking reaction of the PDMS matrix is shown in Scheme 1.

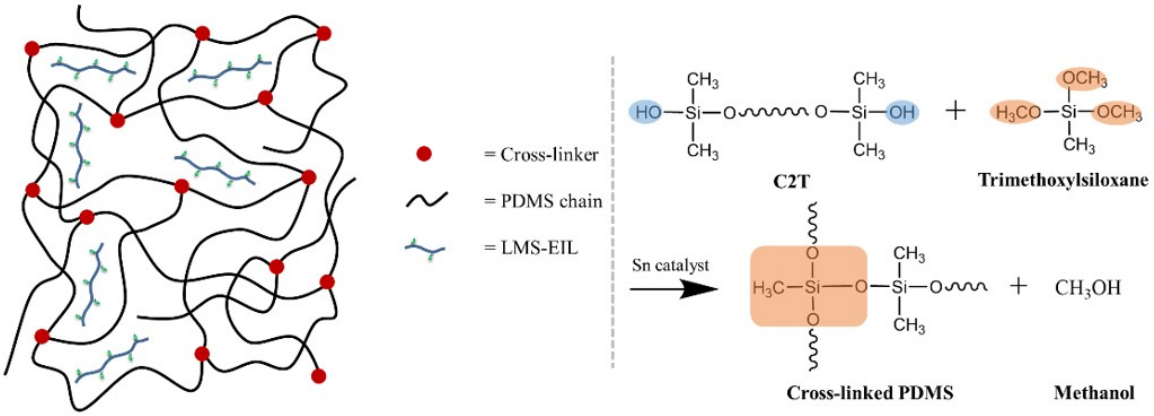

Scheme 1: Cross-linked elastomer incorporated with LMS-EIL in PDMS matrix and reaction between silanol-terminated PDMS and trimethoxylsiloxane cross-linker.

3.1 ^{1}H-NMR and FT-IR analysis of LMS-EIL

^{1}H-NMR spectra were used to investigate the grafting of IL onto chloropropyl-silicone oil. Figure 1a and b show the spectra acquired for LMS-152 and LMS-EIL, respectively. Since there are electronegative atoms (N) and unsaturated groups on the cation of IL (imidazole)[25], the chemical shifts of hydrogens on imidazole move down field. As can be seen in Figure 1b, the corresponding chemical shifts of hydrogens on the imidazole structure are visible on the spectrum, with peaks at 9, 10, and 11 down field. This indicates that the imidazole-based IL has been grafted successfully through nucleophilic substitution[26]. However, the peaks at 5 and 6 in Figure 1b represent the chemical shifts of hydrogen on carbon 5 and 6, respectively, indicating the presence of chloropropyl groups and grafted IL groups in the molecular structure of LMS-EIL. The structure of LMS-EIL was shown on Figure 1b, the number of hydrogens on carbon 5 and 6 can be considered as 2·i and 2·j, respectively. Due to the area under each peak is proportional to the number of hydrogens generating that peak. The grafting ratio (G) of IL is calculated by equation (3):

$$G = j/(i+j)\times 100\% = A_6/(A_5+A_6)\times 100\% \quad (3)$$

Where A_5, A_6 represent the areas below peaks 5 and 6, respectively. Through calculations, the G of IL in LMS-EIL is 30%.

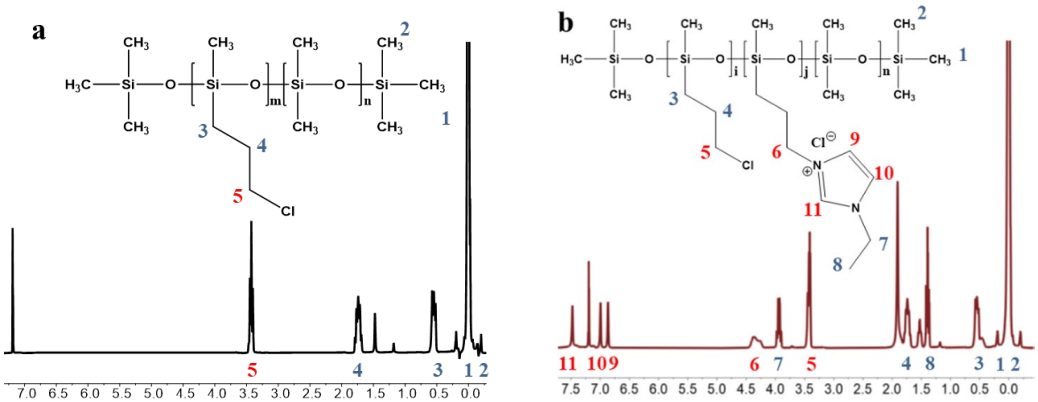

Figure 1: ^{1}H-NMR spectra of LMS-152 (a) and LMS-EIL (b).

As shown in Figure 2, LMS-EIL displays the characteristic peaks of an imidazole ring at 1508 cm^{-1}, which could potentially be regarded as further proof of successful IL-grafting. Because of the low grafting ratio, however, the intensity of the peak at 1508 cm^{-1} is relatively low for LMS-EIL.

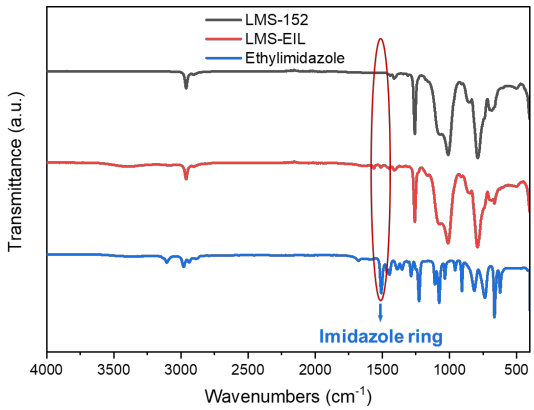

Figure 2: FT-IR spectra of LMS-152, LMS-EIL, and ethylimidazole.

3.2 Dielectric properties of LMS-EIL

Because LMS-EIL is used to modify PDMS elastomers, its initial relative dielectric permittivity strongly affects the resultant elastomers. Figure 3 shows the relative dielectric permittivity (ε_r) and loss tangent (tanδ) of LMS-EIL and LMS-152, respectively. ε_r and tanδ of both compounds at 10^{-1} and 10^6 Hz are presented in Table 1. Compared to that of the pure

silicone oil LMS-152, the ε_r of LMS-EIL increases approximately 9×10^4 times at 10^{-1} Hz. The drastic increase observed in ε_r is clearly the result of the presence of IL, which possesses a much higher relative dielectric permittivity[21] compared to silicone. As expected, ε_r is also seen to decrease in line with increasing frequency, reflecting the leveling off of polarization, since dipoles fail to follow the rapid alternation of the electrical field[27]. It should be noted that the tanδ of LMS-EIL is 30 times lower compared to LMS-152 at 0.1 Hz. Since increases in relative dielectric permittivity are generally followed by large increases in loss tangent, the loss tangent will usually increase. However, LMS-EIL shows a decrease in loss tangent. The dielectric properties of high relative dielectric permittivity and low loss tangent make LMS-EIL potential candidates to be used as additives to modify PDMS elastomers.

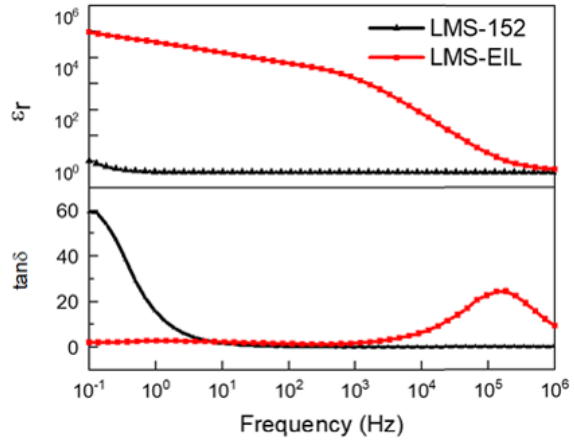

Figure 3: Relative permittivity (ε_r) and loss tangent (tanδ) of LMS-152 and LMS-EIL.

Table 1: Relative permittivity (ε_r) and loss tangent (tanδ) of LMS-152 and LMS-EIL.

Sample	ε_r @ 10^{-1} Hz	ε_r @ 10^6 Hz	tanδ @ 10^{-1} Hz	tanδ @ 10^6 Hz
LMS-152	10.6	3.88	59.2	10^{-5}
LMS-EIL	9.56×10^5	5.16	1.99	9.22

3.3 Morphology of PDMS elastomers incorporated with LMS-EIL

We investigated the morphology of the elastomers using an optical microscope. Figure 4 shows the cross-sectional images of pure elastomer as well as elastomers incorporated with different amounts of LMS-EIL. The elastomers incorporated with 5 and 10 phr LMS-EIL clearly display uniform morphologies comparable to that of the pure elastomer, indicating that LMS-EIL is well dispersed in their elastomer networks. However, LMS-EIL droplets are clearly visible in the elastomer incorporated with 15 phr LMS-EIL—the result of aggregation having taken place.

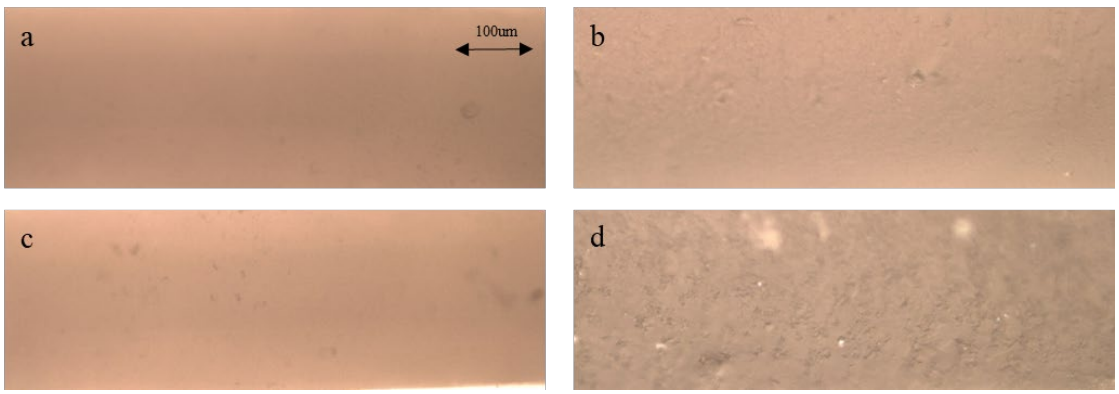

Figure 4: Cross sectional images of elastomers: (a) pure elastomer, (b) elastomer incorporated with 5 phr LMS-EIL, (c) elastomer incorporated with 10 phr LMS-EIL, (d) elastomer incorporated with 15 phr LMS-EIL.

3.4 Dielectric properties of PDMS elastomers incorporated with LMS-EIL

PDMS elastomers incorporated with different amounts of LMS-EIL were prepared to determine the effect of LMS-EIL content on the ε_r and tanδ of the resulting modified elastomers. As the comparison with the pure elastomer in Figure 5a clearly illustrates, there is an obvious increase in ε_r with increased LMS-EIL content. Moreover, at frequencies below 100Hz, the elastomers incorporated with both 10 and 15 phr LMS-EIL display noticeable plateaus in ε_r—consistent with the dielectric behavior of the LMS-EIL additive shown in Figure 3. As noted in Table 2, at 10^{-1} Hz, compared to the pure elastomer, ε_r increases from 2.98 to 3.34 and 22.3, respectively, for elastomers incorporated with 10 phr of LMS-152 or LMS-EIL—indicating that, as expected, it is more efficient to modify elastomers with IL-grafted silicone rather than chloropropyl-silicone. Tanδ values of the elastomers incorporated with 5 and 10 phr LMS-EIL are 0.07 and 0.06 at 10^{-1} Hz, respectively, lower than that of both the pure elastomer and the elastomer incorporated with LMS-152. This can be explained by the fact that LMS-EIL displays a low loss tangent at low frequency, as seen in Figure 3, which decreases the tanδ of the resulting elastomers. Nevertheless, when the LMS-EIL content is further increased, the tanδ of the resulting elastomers increases above that of both the pure elastomer and the elastomer incorporated with LMS-152.

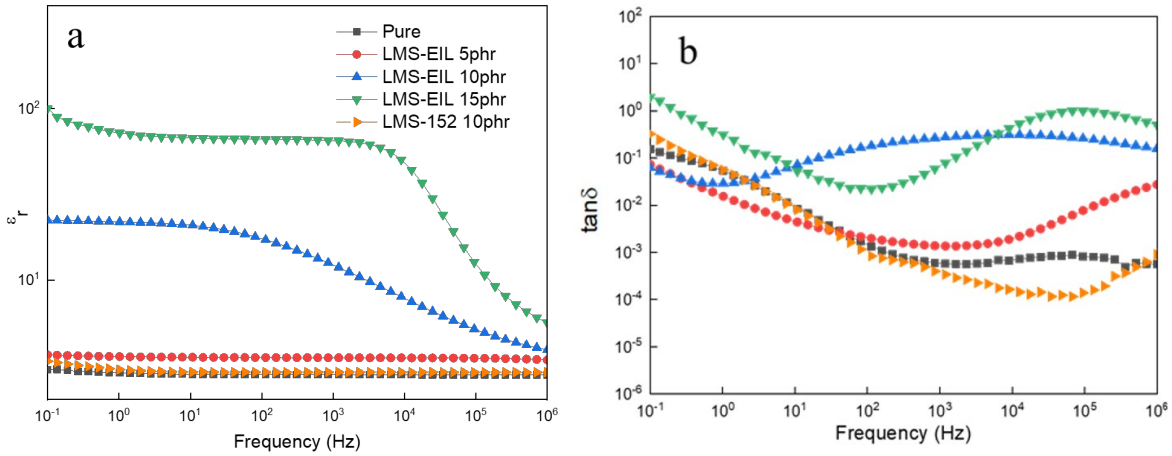

Figure 5: Relative dielectric permittivity (a) and loss tangent (b) of elastomers with different amounts of LMS-EIL.

Table 2: Relative dielectric permittivity (ε_r) and loss tangent (tanδ) of elastomers.

Sample	ε_r @ 10^{-1} Hz	ε_r @ 10^6 Hz	tanδ @ 10^{-1} Hz	tanδ @ 10^6 Hz
Pure	2.98	2.79	0.15	5.56×10^{-4}
LMS-EIL-5phr	3.65	3.41	0.07	0.02
LMS-EIL-10phr	22.3	3.90	0.06	0.16
LMS-EIL-15phr	100	5.61	1.96	0.50
LMS-152-10phr	3.34	2.89	0.59	6.69×10^{-4}

3.5 Mechanical properties of PDMS elastomers incorporated with LMS-EIL

Tensile testing was performed to evaluate the mechanical properties of PDMS elastomers incorporated with different amounts of LMS-EIL. Table 3 lists the Young's modulus and tensile strength for all elastomers studied, both of which are highest in the pure elastomer, as both of these values tend to decrease with the increasing LMS-EIL content due to softening effect of the additive on the elastomer and dilution of the network[17]. Importantly, a decreased Young's modulus is favorable for actuation. In addition to improving relative dielectric permittivity, LMS-EIL also functions as a softening oil. The elastomers incorporated with 10 phr LMS-152 or LMS-EIL have very similar Young's modulus and tensile strength, indicating that both of the additives perform no significant difference to softening the elastomers. As can be seen in Table 3, the elastomer incorporated with 10 phr LMS-EIL exhibits the highest tensile strain of the tested specimens. Nevertheless, the elastomer incorporated with 10 phr LMS-EIL has better overall mechanical properties due to a combination of inherent softness and sufficiently high tensile strain.

Table 3: Mechanical properties of elastomers with different amounts of LMS-EIL.

Sample	$Y_{0\text{-}10\%strain}$ (MPa)	Tensile strain (%)	Tensile strength (MPa)
Pure	0.88±0.04	236±5	0.69±0.12
LMS-EIL-5phr	0.84±0.09	281±8	0.63±0.12
LMS-EIL-10phr	0.78±0.01	321±11	0.54±0.04
LMS-EIL-15phr	0.73±0.02	230±3	0.42±0.01
LMS-152-10phr	0.76±0.02	240±24	0.56±0.07

3.6 Electric breakdown and figure of merit for actuators

Modified elastomers' electric breakdown strength (E_{BD}) was tested and the simplified figure of merit (F_{om}') was calculated to evaluate DEA performance. Table 4 shows the E_{BD} and F_{om}' for all elastomers studied. The E_{BD} of elastomers incorporated with LMS-EIL decreased with increasing LMS-EIL content. F_{om}' was calculated in order to evaluate the improved actuation performance. As seen in Equation (2), an elastomer's F_{om}' is governed by the combination of ε_r and Y. Higher ε_r and lower Y will result in a higher F_{om}'. As seen in both Figure 5 and Table 3, the incorporation of LMS-EIL helps to increase elastomers' ε_r while simultaneously decreasing Y. Additionally, the F_{om}' of the elastomer incorporated with 10 phr LMS-EIL was shown to be 5.4 times higher than that of the elastomer incorporated with LMS-152, indicating that materials incorporated with LMS-EIL display high potential for use as actuators. Due to the aggregation detected in the elastomer incorporated with 15 phr LMS-EIL, the rough morphology and the lowest E_{BD} diminish its potential use as an actuator. Thus, upon an overall evaluation, elastomers incorporated with 10 phr LMS-EIL provided the best potential for actuation applications among those studied here.

Table 4: Electric breakdown strength and figure of merit of elastomers with different amounts of LMS-EIL.

Sample	E_{BD} (V μm^{-1})	F_{om}'
Pure	69±6.0	1.00
LMS-EIL-5phr	25±2.0	1.22
LMS-EIL-10phr	20±0.9	8.06
LMS-EIL-15phr	17±0.6	38.6
LMS-152-10phr	34±0.4	1.49

4. CONCLUSIONS

We successfully synthesized a novel, PDMS elastomer-compatible soft additive, LMS-EIL, by grafting imidazole-based IL to chloropropyl functional silicone at a grafting ratio of 30%. The relative dielectric permittivity of LMS-EIL is 9×10^4 times higher than that of the chloropropyl functional silicone oil (LMS-152), and the loss tangent of LMS-EIL is 30 times lower than that of LMS-152 at 0.1Hz. We also synthesized high-permittivity elastomers through the incorporation of LMS-EIL in varying concentrations. In addition to displaying a uniform morphology, the elastomer incorporated with 10 phr LMS-EIL showed a significantly improved relative dielectric permittivity—increasing from 3.0 to 22, compared to the pure film, at 0.1Hz. Elastomers' Young's modulus was shown to decrease steadily with increasing LMS-EIL content. The improvements observed here indicate that LMS-EIL functions as both a high relative permittivity additive and as a softening oil. Finally, the simplified figure of merit (F_{om}') of the elastomer incorporated with 10 phr LMS-EIL was 8.1, indicating excellent potential as an actuator.

ACKNOWLEDGEMENTS

This work is supported by the Department of Chemical and Biochemical Engineering, Technical University of Denmark and Institute of Process Engineering, Chinese Academy of Sciences.

REFERENCES

[1] Brochu, P., Pei, Q., "Advances in dielectric elastomers for actuators and artificial muscles," Macromol. Rapid Commun. 31(1), 10-36 (2011).

[2] Kornbluh, R. D., Pelrine, R., Pei, Q., Heydt, R., Stanford, S., Oh, S., Eckerle, J., "Electroelastomers: applications of dielectric elastomer transducers for actuation, generation, and smart structures," Proc. SPIE 4698, 254-270 (2002).

[3] Madsen, F. B., Daugaard, A. E., Hvilsted, S., Skov, A. L., "The current state of silicone‐based dielectric elastomer transducers," Macromol. Rapid Commun. 37(5), 378-413 (2016).

[4] Perju, E., Shova, S., Opris, D. M., "Electrically driven artificial muscles using novel polysiloxane elastomers modified with nitroaniline push-pull moieties," ACS Appl. Mater. Interfaces 12(20), 23432-23442 (2020).

[5] Moretti, G., Herran, M. S., Forehand, D., Alves, M., Jeffrey, H., Vertechy, R., Fontana, M., "Advances in the development of dielectric elastomer generators for wave energy conversion," Renew. Sust. Energ. Rev. 117, 109430 (2020).

[6] Zhao, H., Hussain, A. M., Israr, A., Vogt, D. M., Duduta, M., Clarke, D. R., Wood, R. J., "A wearable soft haptic communicator based on dielectric elastomer actuators," Soft Robot. 7(4), 451-461 (2020).

[7] Pelrine, R., Kornbluh, R., Pei, Q., Joseph, J., "High-speed electrically actuated elastomers with strain greater than 100%," Science 287(5454), 836-839 (2000).

[8] Qi, D., Zhang, K., Tian, G., Jiang, B., Huang, Y., "Stretchable electronics based on PDMS substrates," Adv. Mater. 33, 2003155 (2020).

[9] Skov, A. L, Yu, L., "Optimization techniques for improving the performance of silicone-based dielectric elastomers," Adv. Eng. Mater. 20(5), 1700762 (2018).

[10] Rosset, S., Shea, H. R., "Small, fast, and tough: Shrinking down integrated elastomer transducers," Appl. Phys. Rev. 3(3), 031105 (2016).

[11] Madsen, F. B., Yu, L., Daugaard, A. E., Hvilsted, S., Skov, A. L., "A new soft dielectric silicone elastomer matrix with high mechanical integrity and low losses," RSC Adv. 5(14), 10254-10259 (2015).

[12] Yu, L., Skov, A. L., "Silicone rubbers for dielectric elastomers with improved dielectric and mechanical properties as a result of substituting silica with titanium dioxide," Int. J. Smart Nano Mater. 6(4), 268-289 (2015).

[13] Yu, L., Skov, A. L., "ZnO as a cheap and effective filler for high breakdown strength elastomers," RSC Adv. 7(72), 45784-45791 (2017).

[14] Wang, W., Xiang, C., Zhu, Q., Zhong, W., Li, M., Yan, K., Wang, D., "Multistimulus responsive actuator with GO and carbon nanotube/PDMS bilayer structure for flexible and smart devices," ACS Appl. Mater. Interfaces 10(32), 27215-27223 (2018).

[15] Zhang, J., Zhao, F., Zuo, Y., Zhang, Y., Chen, X., Li, B., Zhang, N., Niu, G., Ren, W., Ye, Z., "Improving actuation strain and breakdown strength of dielectric elastomers using core-shell structured CNT-Al_2O_3," Compos. Sci. Technol. 200, 108393 (2020).

[16] Hunt, S., McKay, T. G., Anderson, I. A., "A self-healing dielectric elastomer actuator," Appl. Phys. Lett. 104, 113701 (2014).

[17] Shivapooja, P., Cao, C., Orihuela, B., Levering, V., Zhao, X., Rittschof, D., López, G. P., "Incorporation of silicone oil into elastomers enhances barnacle detachment by active surface strain," Biofouling 32(9), 1017-1028 (2016).

[18] Liu, M., Yu, L., Vudayagiri, S., Skov, A. L., "Incorporation of liquid fillers into silicone foams to enhance the electro-mechanical properties," Int. J. Smart Nano Mater. 11(1), 11-23 (2020).

[19] Lei, Z., Chen, B., Koo, Y., MacFarlane, D. R., "Introduction: ionic liquids," Chem. Rev. 117(10), 6633-6635 (2017).

[20] Zhang, S., Sun, J., Zhang, X., Xin, J., Miao, Q., Wang, J., "Ionic liquid-based green processes for energy production," Chem. Soc. Rev. 43(22), 7838-7869 (2014).

[21] Huang, M. M., Weingärtner, H., "Protic ionic liquids with unusually high dielectric permittivities," ChemPhysChem 9(15), 2172-2173 (2008).

[22] Liu, X., Yu, L., Nie, Y., Skov, A. L., "Silicone elastomers with high‐permittivity ionic liquids loading, " Adv. Eng. Mater. 21(10), 1900481 (2019).

[23] Vudayagiri, S., Zakaria, S., Yu, L., Hassouneh, S. S., Benslimane, M., Skov, A. L., "High breakdown-strength composites from liquid silicone rubbers," Smart Mater. Struct. 23(10), 105017 (2014).

[24] Sommer-Larsen, P., Larsen, A. L., "Materials for dielectric elastomer actuators," Proc. SPIE 5385, 68-77 (2004).

[25] Zhang, H., Li, M., Yang, B., "Design, synthesis, and analysis of thermophysical properties for imidazolium-based geminal dicationic ionic liquids," J. Phys. Chem. C 122(5), 2467-2474 (2018).

[26] Kim, D. W., Song, C. E., Chi, D. Y., “Significantly enhanced reactivities of the nucleophilic substitution reactions in ionic liquid,” J. Org. Chem. 68(11), 4281-4285 (2003).
[27] Weingärtner, H., Sasisanker, P., Daguenet, C., Dyson, P. J., Krossing, I., Slattery, J. M., Schubert, T., “The dielectric response of room-temperature ionic liquids: Effect of cation variation,” J. Phys. Chem. B 111(18), 4775-4780 (2007).